21st Australasian Fluid Mechanics Conference
Adelaide, Australia
10-13 December 2018

Numerical Anisotropy of the 2D Linearised Euler Equations under Spatial and Temporal Discretization for a Hybrid Spectral/Finite Difference Method

Raynold Tan, Andrew Ooi and Richard Sandberg

Department of Mechanical Engineering,
University of Melbourne, Parkville VIC 3010, Australia

Abstract

In this paper, a framework for error analysis of numerical schemes in multidimensional wavenumber space under spatial and temporal (full) discretization is introduced. The numerical anisotropy of the two-dimensional advection and compressible Linearised Euler Equations (LEE) was analysed using this framework under different spatial discretisation methods; Fourier spectral (FS), finite difference and hybrid FS/finite difference. For the compressible two-dimensional LEE, it was found that the dispersive error from the use of a finite difference method in one spatial direction can propagate into the spatial direction for which a FS method was employed. This is because, unlike the advection equation, the additional acoustic term within the semi-discretized dispersion relation of the compressible LEE makes the group velocities a function of the modified wavenumbers in both spatial directions.

Introduction

In high accuracy Direct Numerical Simulation (DNS) of turbulence as well as aeroacoustic, there is a need for high order numerical schemes with low dispersive and dissipative properties. Therefore, the assessment of numerical schemes is critical in determining schemes fit for purpose. The use of spectral analysis to determine dispersive (phase) and dissipative (amplitude) error of finite difference schemes in one dimensional wavenumber space is well established and has been extensively studied in [3, 7, 9]. Since the accuracy of the numerical solution is directly dependent on both the spatial and temporal scheme in combination, better ways to assess numerical error under full discretization are desirable. The assessment of numerical schemes under full discretization in one dimensional wavenumber space has been studied in [6]. In the current work, numerical schemes will be assessed in multidimensional wavenumber space under full discretization in order to have a more complete understanding of their accuracy. In particular, the effect of hybrid spatial discretization on dispersive errors for both the advection equation and the compressible LEE is investigated. The starting point of this framework will be on the finite difference method and its associated modified (scaled) wavenumber [4, 9].

Methodology

Finite Difference Method

For linear finite difference methods, the numerical approximation of a spatial derivative can be expressed as follows:

$$\sum_{m=-M}^{M} b_m \left(\frac{d\phi}{dx}\right)_{i+m} = \frac{1}{\Delta x} \sum_{l=-L}^{+L} a_l \phi_{j+l} \,, \qquad (1)$$

where a_l and b_m are coefficients which represent weighting that determines how much each node contributes to the calculation of the derivatives. The application of Fourier transforms to equation (1) [9, 7, 3] leads to an expression for the modified scaled wavenumber ($k_x^*\Delta x$). The real and imaginary part of the modified wavenumber represent the dispersive and dissipative characteristic of the spatial discretization scheme respectively. Dispersive properties of central type schemes such as the sixth order accurate central compact (CCOM6) [3], sixth order accurate central difference (CDS6) as well as the one sided third order accurate backward difference (BDS3) scheme are shown in figure 1. The black solid line represents the ideal case (spectral) for which all scaled wavenumber up to the Nyquist limit are resolved; $k^*\Delta x = k\Delta x$. High resolution spatial schemes such as the CCOM6 scheme are able to match this ideal relation up to a high wavenumber range before their modified wavenumber value starts decreasing. While central schemes are non dissipative, the modified wavenumber of the third order accurate backward difference (BDS3) scheme has an imaginary component which makes it inherently dissipative.

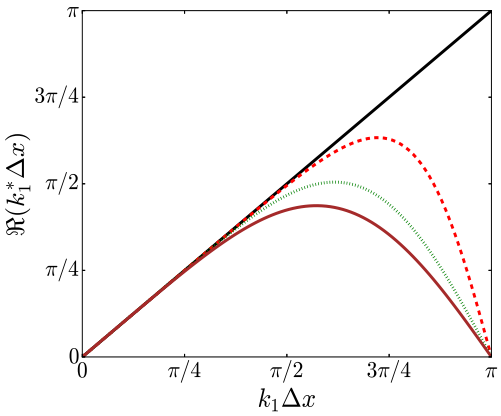

Figure 1: Real component of the modified wavenumber relation for: - - - CCOM6, ····· CDS6, —— BDS3, —— Spectral

Fourier Spectral Method

In FS method, the governing equations are transformed into Fourier space using discrete Fourier transforms. Considering a one dimensional inverse Fourier transform of the variable, ϕ in a [0,2π] domain, a first order spatial derivative in Fourier space can be expressed as follows [1]:

$$F_\kappa\{\frac{d\phi}{dx}\}_j = F_\kappa \left\{ i\kappa \sum_{\kappa=-N/2}^{N/2-1} \hat{\phi}_\kappa e^{i\kappa x_j} \right\} = i\kappa\, \hat{\phi}_j, \qquad (2)$$

where $j = 0.....N-1$. N represent the total number of points in the discretized domain. FS method does not produce any dispersive error because the actual Fourier transform of the spatial derivative is being used in the numerical calculation. As such, it is able to achieve ideal spectral accuracy ($k^*\Delta x = k\Delta x$). However, Fourier series are limited to periodic functions and not suited for functions characterised by sharp discontinuity such as shockwaves. Since the FS method can numerically resolve solutions up to a high wavenumber, high frequency spurious oscillation in the interpolation around sharp gradients of discontinuities can get amplified, leading to numerical instability.

Full Discretization Analysis

For simplicity, the two-dimensional advection equation will be used to illustrate the extension of linear spectral analysis of spatial discretization scheme into full discretization framework.

Thereafter, the dispersion relation of the two-dimensional LEE will be introduced, from which the analysis will be extended. In all of the analysis in this section, it is assumed that $\Delta x = \Delta y$.

2D Advection

The two-dimensional advection equation can be written as follows:

$$\frac{\partial \phi}{\partial t} + \bar{u}\frac{\partial \phi}{\partial x} + \bar{v}\frac{\partial \phi}{\partial y} = 0. \tag{3}$$

By expressing ϕ in terms of its inverse Fourier transform and taking its derivative with respect to x, y and t, the two-dimensional advection equation can be simplified to the following form [9]:

$$\frac{\partial}{\partial t}\hat{\phi}(k_1,k_2,t) = -\bar{u}ik_1^*\hat{\phi}(k_1,k_2,t) - \bar{v}ik_2^*\hat{\phi}(k_1,k_2,t), \tag{4}$$

from which the modified wavenumbers, k_1^* and k_2^* are introduced into the spatial derivative terms due to the finite difference approximation. In order to perform analysis on the full discretization scheme, the solution in Fourier space must be advanced through time using a numerical time marching scheme. In this work, the fourth order accurate explicit Runge Kutta time (RK4) discretization method [4] was used for the analysis and simulation. Substituting the right hand side of equation (4) into the RK4 time discretization equation leads to the following expression [2]:

$$\frac{\hat{\phi}^{n+1}}{\hat{\phi}^n} = \Big[1 - (\Delta t i\omega^*_{semi}) + \frac{(\Delta t i\omega^*_{semi})^2}{2} - \frac{(\Delta t i\omega^*_{semi})^3}{6} + \frac{(\Delta t i\omega^*_{semi})^4}{24}\Big], \tag{5}$$

where $\omega^*_{semi} = \bar{u}k_1^* + \bar{v}k_2^*$ represents the semi-discretized dispersion relation of the two-dimensional advection equation. The term in the square bracket is the numerical amplification factor, Z which now contains information on the numerical error due to both the spatial and temporal discretization schemes. The CFL number, $R = \frac{\bar{u}\Delta t}{\Delta x} = 0.1$ which is used within the numerical amplification factor as a proxy for the time step is kept to a small value in order to neglect the effect of temporal discretization. Z is a complex number, that can be expressed as $Z = |Z|e^{-i\Psi}$, where $|Z| = \sqrt{\Re(Z)^2 + \Im(Z)^2}$ and $\Psi = -\arctan(\frac{\Im(Z)}{\Re(Z)})$. A measure of the dispersive and dissipative error under full discretization is to consider the numerical group velocity and the absolute magnitude of the numerical amplification factor, $|Z|$. Ψ represents the phase shift of the amplification factor. The numerical group velocity is formulated as follows [2]:

$$U^*_{grp} = \frac{1}{\Delta t}\frac{\partial \psi}{\partial k_1}, \quad V^*_{grp} = \frac{1}{\Delta t}\frac{\partial \psi}{\partial k_2}. \tag{6}$$

The y component of the normalised group velocities ($V^*_{grp}/v^{exact}_{grp}$) in two-dimensional wavenumber space for the CDS6 scheme is plotted in figure 2. V^*_{grp} is considered for this analysis in order to have a consistent comparison with the results of the LEE in the next section. The value of $\bar{u} = \bar{v} = 0.5$ is kept to the same. For the advection equation, the exact solution of the group velocity, v^{exact}_{grp} is 0.5. As seen in figure 2, the normalised group velocity ($V^*_{grp}/v^{exact}_{grp}$) is only governed by the differencing scheme used in the $k_2\Delta y$ direction since there is no variation in the $k_1\Delta x$ direction. Figure 2 is also valid for the hybrid FS/CDS6 discretization case where the CDS6 scheme is used in the y direction. $V^*_{grp}/v^{exact}_{grp}$ is only dependent on the discretization scheme used in the y direction. The normalised group velocity results of the FS/FS and CDS6/FS discretization case are presented in table 1. For cases where FS method is used in the y direction, the normalised group velocity becomes 1.0 for all wavenumbers. A summary of the results for all the different spatial discretization method is shown in table 1.

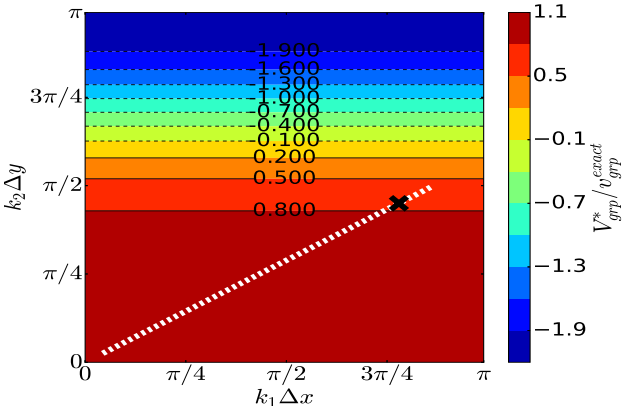

Figure 2: $V^*_{grp}/v^{exact}_{grp}$ in $k_1\Delta x - k_2\Delta x$ plane for the case: a) CDS6 scheme applied in the x and y direction (CDS6/CDS6), b) FS method applied in the x and CDS6 scheme applied in the y direction (FS/CDS6). RK4 temporal scheme. Black cross represents the solution ($V^*_{grp}/v^{exact}_{grp} = 0.734$) corresponding to an initial condition of $k\Delta = \frac{9\pi}{10}$ and wave propagation angle, $\theta_w = 30°$.

Case	Spatial discretization	$V^*_{grp}/v^{exact}_{grp}$
a	CDS6 in x, y (CDS6/CDS6)	figure 2
b	FS in x, CDS6 in y (FS/CDS6)	figure 2
c	CDS6 in x, FS in y (CDS6/FS)	1.0 for all $k_1\Delta x$, $k_2\Delta y$
d	FS in x, y (FS/FS)	1.0 for all $k_1\Delta x$, $k_2\Delta y$

Table 1: $V^*_{grp}/v^{exact}_{grp}$ for advection eq.

Compressible 2D Linearized Euler Equations

The compressible formulation of the two-dimensional LEE in conservative form can be expressed as follows:

$$\frac{\partial \mathbf{U}}{\partial t} + \frac{\partial \mathbf{E}}{\partial x} + \frac{\partial \mathbf{F}}{\partial y} = \mathbf{0}, \tag{7}$$

where

$$\mathbf{U} = \begin{bmatrix} \rho' \\ u' \\ v' \\ p' \end{bmatrix} \quad \mathbf{E} = \begin{bmatrix} \bar{u}\rho' + \bar{\rho}u' \\ \bar{u}u' + p'/\rho \\ \bar{u}v' \\ \rho a^2 u' + \bar{u}p' \end{bmatrix} \quad \mathbf{F} = \begin{bmatrix} \bar{v}p' + \bar{\rho}v' \\ \bar{v}u' \\ \bar{v}v' + p'/\rho \\ \rho a^2 v' + \bar{v}p' \end{bmatrix}. \tag{8}$$

Field variables denoted with $(..)'$ represent the perturbed field while those with $\overline{(..)}$ represent the time averaged field. By applying a Fourier Laplace transform to the conservative variables, $\mathbf{U}$ and solving for their eigenvalues, it can be shown that the dispersion relation of the two-dimensional LEE reduces to the following form [5]:

$$\omega = \underbrace{\bar{u}k_1 + \bar{v}k_2}_{advective} + \underbrace{\alpha a\sqrt{(k_1)^2 + (k_2)^2}}_{acoustic}, \tag{9}$$

where α takes on the value of 1, -1 and 0 depending on the eigenvalues sought for. The value of α will be taken as 1 for the analysis used in this work. a represents the speed of sound. Analogous to the advection equation, spatial discretization effects are taken into account via the modified scaled wavenumber, $k^*\Delta = f(k\Delta)$. The semi-discretized form of the dispersion relation can be expressed as follows:

$$\omega^*_{semi} = \underbrace{\bar{u}k_1^* + \bar{v}k_2^*}_{advective} + \underbrace{\alpha a\sqrt{(k_1^*)^2 + (k_2^*)^2}}_{acoustic}. \tag{10}$$

In equation (10), the first two terms on the right hand side are the same as those of the advection equation and they represent the advective term. The last term on the right hand side represents the acoustic term. The significance of this term under a hybrid discretization framework can be better understood if the group velocities are computed under the consideration of spatial discretization effects [5, 8]. The y component of the group velocity (V^*_{grp}) was selected for this analysis as the propagation of dispersive error from the discretization scheme used in the x direction is more pronounced. The group velocity (V^*_{grp}) under spatial discretization effects can be expressed as follows:

$$(V^*_{grp}) = \frac{\partial \omega^*_{semi}}{\partial k_2} = \Big[\underbrace{\bar{v}}_{advective} + \underbrace{\frac{\alpha a}{\sqrt{(\frac{k^*_1}{k^*_2})^2 + (1)^2}}}_{acoustic} \Big] \frac{\partial k^*_2}{\partial k_2}. \quad (11)$$

A similar expression can be derived for U^*_{grp}. While the advection equation contains only the advective term, the group velocities (U^*_{grp} and V^*_{grp}) of the LEE are a function of the modified wavenumbers in both spatial directions as a result of the acoustic term. The contribution of the acoustic term becomes significant when the ratio of $\frac{k^*_1}{k^*_2}$ becomes small. The normalised group velocity ($V^*_{grp}/v^{exact}_{grp}$) in two-dimensional wavenumber space for the CDS6/CDS6 case is plotted in figure 3. The values of $\bar{u}$ and $\bar{v}$ are set to 0.5 and 0.0 respectively. By keeping $\bar{v} = 0$, the group velocity (V^*_{grp}) error originating solely from the acoustic term can be analysed. As before, the CFL number ($R_a = \frac{a\Delta t}{\Delta x} = 0.1$), in terms of the speed of sound, a is kept to a small value. The group velocities are computed according to equation (6) using the numerical amplification factor from equation (5) and the semi discretized dispersion relation from equation (9).

Unlike the advection equation, the normalised group velocity of the LEE under different spatial discretization methods showcases variation in both spatial directions as a result of the additional acoustic term. A summary of the results is shown in table 2 and figure 3. The FS/FS case (figure 3b) represents the exact solution of the system. While the exact solution of the advection equation has a constant group velocity (V^*_{grp}) value of 0.5 for all scaled wavenumbers and wave propagation angle, θ_w, the exact solution of the LEE varies according to θ_w. As seen in figure 3b, a change in the angle of the dotted line about the origin (0,0) for a given $k\Delta$ gives a different group velocity. For an initial condition of $k\Delta = \frac{9\pi}{10}$ and $\theta_w = 30°$, a faster normalised group velocity was found in both the hybrid CDS6/FS case (figure 3c, $V^*_{grp}/v^{exact}_{grp} = 1.506$) and the CDS6/CDS6 discretization case (figure 3b, $V^*_{grp}/v^{exact}_{grp} = 1.08$) than the exact solution ($V^*_{grp}/v^{exact}_{grp} = 1.0$). The exact group velocity (v^{exact}_{grp}) is found to be 0.503. Also, the result of the CDS6/CDS6 case is more accurate than in the hybrid CDS6/FS case.

Case	Spatial discretization	$V^*_{grp}/v^{exact}_{grp}$
a	CDS6/CDS6	figure 3a
b	FS/FS	figure 3b
c	CDS6/FS	figure 3c

Table 2: $V^*_{grp}/v^{exact}_{grp}$ for LEE

Numerical Set-up

Numerical variables are marched in time using a small CFL number with the fourth order accurate Runge Kutta time integration scheme. Spatial derivatives are computed using the CDS6 scheme, FS method solely or both methods in combination. In the hybrid discretization case, the CDS6 scheme is applied in the x and the FS method is applied in the y direction. Periodic boundary conditions are imposed at all edges of the domain. A 300 $\times$ 300 grid is used for all numerical experiments. For the advection equation, $\bar{u} = \bar{v} = 0.5$. For the LEE, $\bar{u}$ and $\bar{v}$

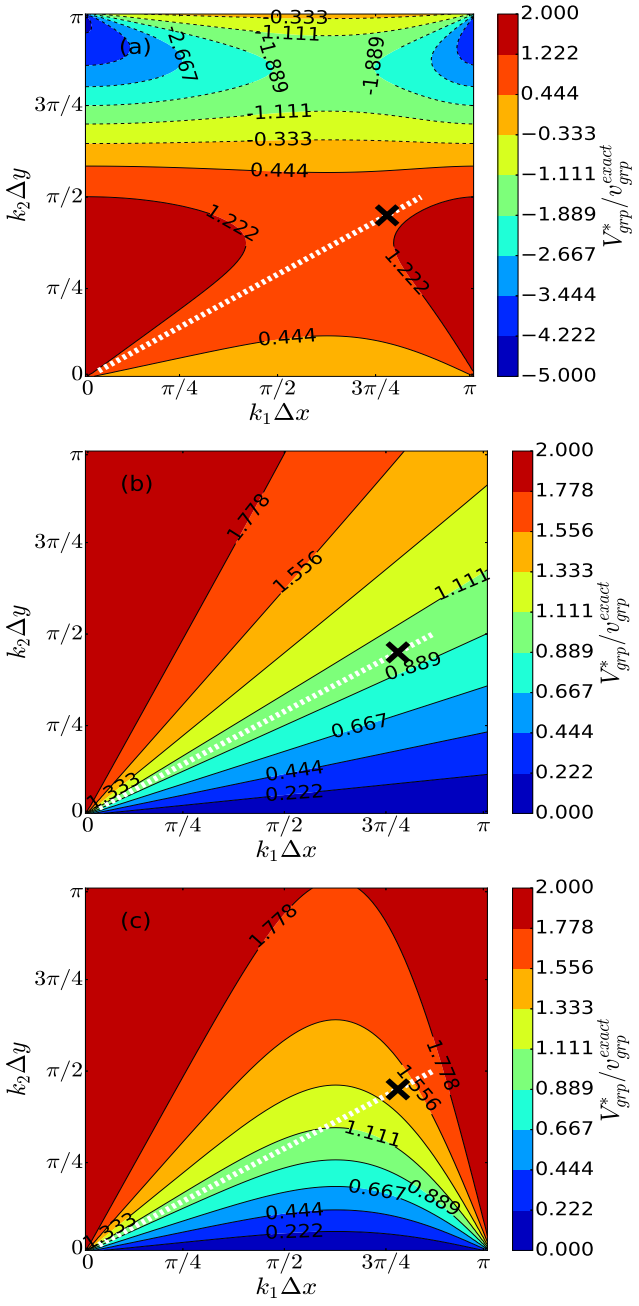

Figure 3: $V^*_{grp}/v^{exact}_{grp}$ in $k_1\Delta x - k_2\Delta x$ plane for the case: a) CDS6/CDS6 b) FS/FS (exact solution) c) CDS6/FS, $\alpha = 1$ and RK4 temporal scheme. Black cross represents the solutions ($V^*_{grp}/v^{exact}_{grp} = 1.082, 1.0, 1.506$) corresponding to an initial condition of $k\Delta = \frac{9\pi}{10}$ and $\theta_w = 30°$ for figures a,b,c.

are set to 0.5 and 0 respectively. The density, $\bar{\rho}$, is set to 1.0 for the LEE. For both equations, the prescribed initial conditions are as follows:

$$\phi(x, y, 0) = e^{-0.5(x^2+y^2)} \sin(k_1 x + k_2 y), \quad (12)$$

where $k_1 = k\cos(\theta_w)$ and $k_2 = k\sin(\theta_w)$. θ_w represents the initial orientation of the wave front with respect to the grid. A value of $\theta_w = 30°$ and $k\Delta = \frac{9\pi}{10}$ was prescribed. In the case of the LEE, ϕ represents the perturbed pressure variable and all other variables are set to zero initial condition. The wave packet is centered at the origin (0,0) at $t = 0$. A large value of $k\Delta$ was used in order to illustrate the dispersion error.

Results

In this section, the results of the analysis are compared to numerical experiments. For the advection equation, the normalised group velocities of the different cases are presented in table 3. The numerical and analytical group velocity results are illustrated in figure 4. The numerical results are shown by the shaded wave packets and the coloured arrows show the location of the wave packets predicted by the group velocities. It can be seen that y_{pos} of the wave packet of the CDS6/FS case (blue arrow) matches the solution of the FS/FS case (black arrow) even though the x_{pos} of the wave packets does not match. This implies that the dispersion error arising from the CDS6 scheme applied in the x direction has no effect on V^*_{grp}. This is because the group velocity computed in one spatial direction is only governed by the gradient of the modified wavenumber and the advection velocity in the spatial direction considered (e.g. $V^*_{grp} = \bar{v}\frac{\partial k^*_2}{\partial k_2}$).

Spat. discret.	$U^*_{grp}/u^{exact}_{grp}$	$V^*_{grp}/v^{exact}_{grp}$	x_{pos}	y_{pos}
CDS6/CDS6	-1.315	0.733	-1.315	0.733
FS/FS	1.0	1.0	1.0	1.0
CDS6/FS	-1.315	1.0	-1.315	1.0

Table 3: Group velocities and location of wave packet at t=2 for advection eq, $u^{exact}_{grp} = 0.5$, $v^{exact}_{grp} = 0.5$.

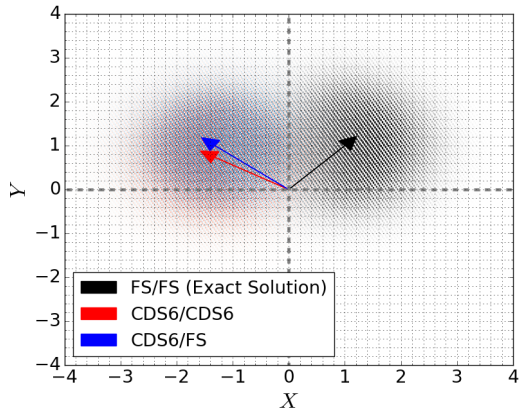

Figure 4: Location of wave packets at t=2 for different spatial discretization methods for $k\Delta = \frac{9\pi}{10}$ and $\theta_w = 30°$.

For the LEE, the normalised group velocities of the different discretization cases are presented in table 4. These results are illustrated in figure 5. For the prescribed initial condition, there exist two wave packets ($\alpha = 1, -1$) travelling in different directions. For conciseness, only the solution for $\alpha = 1$ is shown. As before, the numerical results match the solution of the group velocities (coloured arrows). For the LEE, the y_{pos} of the wave packet of the CDS6/FS case (blue arrow) is greater than the y_{pos} of the FS/FS case (black arrow). This implies that dispersive errors from the CDS6 scheme applied in the x direction affect V^*_{grp}. Also, it can be seen that the y_{pos} of the CDS6/CDS6 case is more accurate than the CDS6/FS discretization case when compared to the exact solution.

Spat. discret.	$U^*_{grp}/u^{exact}_{grp}$	$V^*_{grp}/v^{exact}_{grp}$	x_{pos}	y_{pos}
CDS6/CDS6	-1.125	1.081	-3.074	1.088
FS/FS	1.0	1.0	2.732	1.01
CDS6/FS	-1.11	1.503	-3.032	1.512

Table 4: Group velocities and location of wave packet at t=2 for LEE, $u^{exact}_{grp} = 1.366$, $v^{exact}_{grp} = 0.503$.

Conclusions

For the advection equation, the dispersive error originating from the finite difference scheme used in the x direction has no influence on V^*_{grp}. For the LEE, the dispersive error originating from the spatial differencing scheme used in the x direction has an influence on V^*_{grp}. It was found that the error in y_{pos} originating from the dispersive error of the finite difference scheme used in the x direction becomes significant when $k\Delta \gtrsim 0.7\pi$ for $\theta_w = 30°$. In contrast to commonly held belief that a hybrid Fourier spectral/finite difference scheme would generally give better numerical resolution characteristic than a full finite difference scheme, it was found that this is only true for the two-dimensional advection equation for all values of $k\Delta$. In the case of the LEE, it was shown that the numerical solution of the hybrid CDS6/FS discretization case is less accurate than the CDS6/CDS6 case for values of large $k\Delta$.

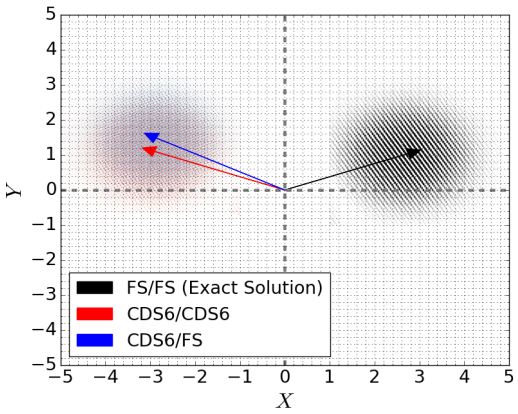

Figure 5: Location of wave packets at t=2 for different spatial discretization methods for $k\Delta = \frac{9\pi}{10}$ and $\theta_w = 30°$. Only the solution for $\alpha = 1$ is plotted

Acknowledgements

Raynold Tan would like to acknowledge the University of Melbourne for supporting his candidature for Doctor of Philosophy in Engineering.

References

[1] Canuto, C., Hussaini, M.Y., Quateroni, A., Zang, T.A., *Spectral Methods, Fundamental in Single Domains*, Springer-Verlag Berlin Heidelberg, 2006.

[2] Durran, D., *Numerical Methods for Wave Equations in Geophysical Fluid Dynamics*, Springer, New York, 1999.

[3] Lele, S.K., Compact finite difference schemes with spectral-like resolution, *J. Comput. Phys.*, **103**, 1992, 16-42.

[4] Moin, P., *Fundamentals of Engineering Numerical Analysis*, Cambridge University Press, Cambridge, 2001. 1963.

[5] Stegeman, P., Young, M., Soria, J. and Ooi, A. Analysis of the anisotropy of group velocities due to spatial finite difference schemes from the solution of the 2D LEE, *J. Comput. Phys.*, **71**, 2013, 235-255.

[6] Suman, V.K., Sengupta, T.K., Prasad, C.J.D. and Mohan,K.S., 17. Spectral analysis of finite difference schemes for convection diffusion equation, *J. Comput. & Fluids*, **150**, 2017, 95-114.

[7] Tam, C. and Webb, J., Dispersion relation preserving finite difference schemes for computational acoustics, *J. Comput. Phys.*, **107**, 1993, 262-281.

[8] Trefethen, L., Group velocity in finite difference schemes, *SIAM Review*, **24**, 1982, 113-136.

[9] Vichnevetsky, R. and Bowles, J., *Fourier Analysis of Numerical Approximation of Hyperbolic Equations*, SIAM, Philadelphia, 1982.